Monatsh Chem (2016) 147:391–403
DOI 10.1007/s00706-015-1616-3

ORIGINAL PAPER

Aerobic oxidation of alcohols on Au/TiO_2 catalyst: new insights on the role of active sites in the oxidation of primary and secondary alcohols

Floriana Vindigni[1] · Stefano Dughera[2] · Francesco Armigliato[2] · Anna Chiorino[2]

Received: 17 September 2015 / Accepted: 23 November 2015 / Published online: 15 December 2015
© Springer-Verlag Wien 2015

Abstract A study of secondary, benzylic, and primary alcohols oxidation on a reference Au/TiO_2 catalyst is reported. Reactions gave rise to ketones, aldehydes, or esters in good yields. The FT-IR results and catalytic tests data provide to elucidate the reaction mechanism and the specific role of the active sites on titania.

Graphical abstract

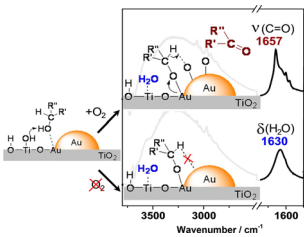

Keywords Alcohol · Oxidation · Gold · Reaction mechanism · FT-IR

Introduction

Gold catalysis has become a particularly active area of research within only a few years. In particular, the last decade has witnessed a remarkable growth in the number of organic reaction that are catalyzed by gold complexes such as oxidative processes [1–4], hydrogenations [5–8], cross-couplings [9–12], and others [13–15].

Selective oxidation of alcohols plays key role in organic synthesis and in industrial practice. The application of heterogeneous catalysis and molecular oxygen [16] to oxidation reactions offers a green alternative to traditional, toxic chemical oxidants. Supported gold nanoparticles (Au NPs) are a means of carrying out alcohol oxidation reactions under mild and green conditions.

It must be stressed that the catalytic activity of gold is remarkably sensitive to many factors, such as gold particle size, preparation method, and support. In particular, the nature of the support can play a key role in its catalytic activity; in fact a number of metal oxides such as CeO_2 [17], TiO_2 [18, 19], mesoporous silica [20], Fe_2O_3 [21], NiO [22, 23], MgO [24], metal hydroxides such as $Mg(OH)_2$ [25] and zeolites [26] were used as a support of Au NPs. For example, Au/CeO_2 is able to catalyze the selective oxidation of alcohols to aldehydes or ketones and acids in relatively mild conditions using O_2 as oxidizing agent [17]. On the contrary, the oxidation carried out in the presence of Au/TiO_2 is scarcely studied [18, 19] and often requires harsh reaction conditions (e.g., under high pressure in an autoclave).

In addition, great attention is also being paid to the study of the specific role that active sites play in the oxidation reaction. In this regard, recent works have reported mechanisms based on the activation of oxygen atoms on the gold surface [27]. Furthermore, it is generally accepted

Electronic supplementary material The online version of this article (doi:10.1007/s00706-015-1616-3) contains supplementary material, which is available to authorized users.

✉ Floriana Vindigni
floriana.vindigni@unito.it

✉ Stefano Dughera
stefano.dughera@unito.it

[1] Department of Chemistry, NIS Centre of Excellence, University of Torino, via P. Giuria 7, Turin, Italy

[2] Department of Chemistry, University of Torino, via P. Giuria 7, 10125 Turin, Italy

that the contact boundaries between the gold and the oxide support play an important role in the catalytic mechanism [21]. Therefore, since many factors can influence catalytic activity, i.e., Au dispersion, nature of the support, metal-support interaction, etc., this research topic is still open to further study.

In the light of this, the purpose of our work is to test a reference Au/TiO_2 (AUROliteTM) catalyst, produced by STREM Chemicals Inc., in the oxidation of primary, benzylic, and secondary alcohols. FT-IR and DRUV–Vis spectroscopy were used to investigate its activity and to clarify the specific role that its active sites play in the reaction.

Results and discussion

Oxidation reaction of 1-phenylethanol (1a) and secondary alcohols 1b–1d

Initially, to optimize the reaction conditions, the oxidation of 1-phenylethanol (**1a**) to acetophenone (**2a**) in the presence of the Au/TiO_2 catalyst was studied under varying conditions, as reported in Table 1.

Firstly, two tests were carried out with TiO_2 (Table 1; entry 1) and $NaOH/TiO_2$ (Table 1; entry 2) to demonstrate that gold is the actual catalyst. In both cases, only unreacted **1a** was detected by GC and GC–MS analyses. On the other hand, no **2a** was obtained when the reaction was carried out without base (Table 1; entry 3). In the light of this, it is clear that NaOH, Au/TiO_2, and atmospheric oxygen were necessary to obtain the complete oxidation of **1a**–**2a**. The best conditions are those reported in entry 5 and involve the use of toluene as a solvent and NaOH (3 equivalents) as a base. Note that no **2a** was obtained when carrying out the same reaction under nitrogen flow (Table 1; entry 6), confirming that oxygen is necessary for alcohol oxidation.

It has been reported [28] that Au may leach into the solution during the reaction. We, therefore, stopped the reaction after 12 h and removed the catalyst (Table 1; entry 7). GC analyses showed **1a** and **2a** in almost equivalent amounts. The residue was reacted for a further 12 h, but the reaction still did not complete, demonstrating that this phenomenon did not affect the catalytic performance of the system.

Experiments with lower amounts of NaOH, other bases (Na_2CO_3, Table 1; entry 8), and other solvents (Table 1; entries 12, 13) generally led to unsatisfactory results. It must be stressed that the oxidation of **1a** only partially occurred when bubbling a continuous oxygen flow without NaOH (Table 1; entry 10). In the presence of NaOH (Table 1; entry 11), the reaction was complete after 8 h and **2a** was obtained in excellent yield. Interestingly, also the reaction carried out in neat conditions gave **2a** in good yield (91 %, Table 1; entry 9).

The catalyst was easily recovered at the end of the reactions by simple vacuum filtration and was reused for other two consecutive catalytic cycles and no significant decrease in catalytic activity was observed, as reported in Table A (see Supplementary Material). Alternatively, instead of recovering the catalyst by filtration at the end of the reaction, **2a** was completely removed by extraction with diethyl ether; new **1a** and toluene were then added to the same environment and the reaction was repeated several times. The catalyst was efficient until the sixth consecutive run. The results are reported in Table B (see Supplementary Material).

The high yield and simplicity of the procedure encouraged us to further exploit the generality and the scope of this oxidation, using other secondary alcohols **1**. The results are collected in Table 2. Alcohol **1b** was oxidized in excellent yields with or without toluene (Table 2; entries 1, 2). However, the oxidation of **1c** only occurred without solvent (Table 2; entries 3, 4). No results were obtained with **1d** (Table 2; entry 5).

Spurred on by these encouraging results, a careful FT-IR spectroscopy investigation was carried out to obtain new insight into the interaction between alcohol and the active sites exposed on the catalyst surface.

FTIR characterization

The FT-IR spectra of adsorbed CO at −153 °C, before 1-phenylethanol (**1a**) interaction, on differently treated catalysts are reported in Fig. 1a.

According to the attribution and nomenclature proposed by Hadjiivanov et al. [29], the peaks at 2179 and 2164 cm^{-1} are associated with CO molecules adsorbed onto pentacoordinated Ti^{4+} ions exposed on (010) and (101) faces (γ sites) and those on pentacoordinated Ti^{4+} ions exposed on (001) planes (γ sites), respectively. Moreover, CO adsorption at low temperature also produces a shoulder at 2155 cm^{-1}, attributed to the interaction between the probe molecules and OH groups; this feature is confirmed by the perturbation of the ν (OH) pattern in the 3750–3600 cm^{-1} range (not shown here).

It is evident that the intensity of the band associated with CO-support site interaction is strictly related to the specific thermal pre-treatment that the catalyst was submitted to. In particular, in the spectrum of the sample underwent to the mild treatment (i.e., AuTiDeg) the band intensity is the lowest, indicating that a smaller amount of Ti^{4+} ions are accessible to the probe molecules in this case. These features have been clarified by a comparison of the FT-IR spectra of the samples before the CO inlet (see Fig. S1 in

Table 1 Oxidation of 1-phenylethanol (**1a**)

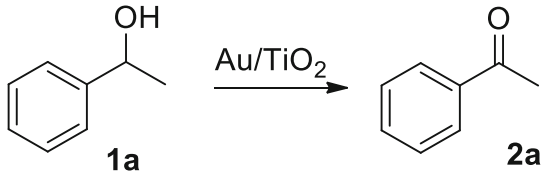

Entry	Solvent	Base (3 eq.)	*T*/°C	Time/h	Yield/% of 2[a, b, c]
1	Toluene	–	110	24	–[d]
2	Toluene	NaOH	110	24	–[d]
3	Toluene	–	110	24	Traces
4	Toluene	Na_2CO_3	110	24	12[e]
5	Toluene	NaOH	110	24	100[f]
6	Toluene	NaOH	110	24	–[g]
7	Toluene	NaOH	110	24	55[h]
8	–	Na_2CO_3	80	48	16
9	–	NaOH	80	72	91[f, i]
10	Toluene	–	110	24	40[j, k]
11	Toluene	NaOH	110	8	100[j]
12	H_2O	NaOH	110	48	Traces
13	MeCN	NaOH	80	48	Traces

[a] All the reactions were carried out with 1 mmol of **1a**, 3 mmol of base, and 50 mg of Au/TiO_2 (equal to 15 mol% of Au)

[b] Yields refer to the pure and isolated **2a**

[c] Note that with lesser amounts of base, the reaction was not complete

[d] The reaction was carried out without catalyst and in the presence of TiO_2 (50 mg)

[e] Unreacted **1a** was also isolated (85 %)

[f] The conversion was total

[g] The reaction was carried out under nitrogen flow

[h] The reaction was stopped after 12 h. GC analyses showed the presence of **1a** and **2a** in almost equivalent amounts. The catalyst was removed and the remaining liquid was heated at 110 °C for further 12 h. After the usual work-up, we obtained an oily residue which was chromatographed on a short silica gel column (eluent: petroleum ether/diethyl ether 9:1). The first eluted product was **2a** (66 mg; 55 % yield); the second one was **1a** (55 mg; 45 %)

[i] The reaction carried out at 110 °C gave lower yield of **2a** (60 %)

[j] The reaction was carried out under a continuous oxygen flow

[k] Unreacted **1a** was also isolated (57 %)

Supplementary Material). These spectra also highlighted the presence of a carbonate-like species and water on the titania surface.

Coming back to the lower frequency range in Fig. 1a, the band centered at 2100 cm^{-1} for AuTiDeg (dotted line) and AuTiRed (solid line) is the stretching mode of CO molecules adsorbed on Au^0 sites. This band has the same intensity on both spectra and indicates that metallic gold sites are available to the reactant after this mild treatment.

However, oxidation treatment gives rise to significant changes in the shape and in the position of the peaks. Particularly, the band due to the CO-Au^0 interaction decreases in intensity and slightly shifts to higher frequency, i.e., 2103 cm^{-1} and, more interestingly, a new broad absorption in the 2130–2120 cm^{-1} region appears. This latter is attributed to the interaction between CO and $Au^{\delta+}$ sites. It is well accepted that the Au sites, particularly those at the metal-support interface, can be made positively charged via bonding with residual active oxygen species which are present after an oxidation pretreatment [28, 30]. Moreover, to further confirm that the intensity decrease of the band due to the CO–Au^0 interaction is not a consequence of an Au particles agglomeration, the same FTIR measurement was undertaken on the Au/TiO_2 submitted to an oxidative treatment at 200 °C (see Fig. S2 in Supplementary Material).

Now, it is necessary to point out that the reactions described above were carried out on "as received" Au/TiO_2 under air atmosphere, while its reactivity will be

Table 2 Oxidation of secondary alcohols **1b–1d**

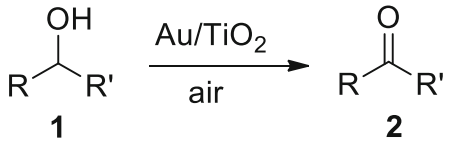

Entry	R	R′	Solvent	*T*/°C	Time/h	Yield/% of **2**[a, b]
1	Ph	Ph (**1b**)	Toluene	110	15	100[c] (**2b**)
2	Ph	Ph (**1b**)	–	80	24	97[c] (**2b**)
3		cC_6H_{11} (**1c**)	Toluene	110	24	– (**2c**)
4		cC_6H_{11} (**1c**)	–	80	52	84[c, d] (**2c**)
5	Me	nC_6H_{13} (**1d**)	–	80	72	– (**2d**)

[a] All the reactions were carried out with 1 mmol of **1**, 3 mmol of NaOH, and 50 mg of Au/TiO_2 (equal to 15 mol% of Au)

[b] Yields refer to the pure and isolated **2**

[c] The conversion was total

[d] The reaction carried out at 110 °C gave lower yield of **2c** (45 %)

investigated by FTIR measurements on AuTiDeg samples, following the operative setup previously reported. This mild thermal pretreatment is necessary, in order to have the catalyst surface adequately clean for FTIR analyses.

In addition, DRUV–Vis spectroscopy and XRD analyses were used to have information on the effect of the thermal treatment on the optical and structural properties of the catalyst (see Fig. S3 and S4 in Supplementary Material). DRUV–Vis spectra (Fig. S3, section A) showed that AuTiDeg and the "as received" Au/TiO_2 are equal. Moreover (Fig. S4), XRD pattern clearly put in evidence that no structural modifications, both the titania and of gold nanoparticles, occurred after the different thermal treatment as well as after the reactions.

The spectra collected after 1-phenylethanol-O_2(a) and 1-phenylethanol/toluene-O_2(b) interactions on the AuTiDeg surface are presented in Fig. 2. For the sake of clarity, we highlight 1750–1000 cm^{-1} range, where the absorption of C=O and C–OH groups is located.

The adsorption of 1-phenylethanol onto the catalyst surface (solid lines, a and b) is confirmed by the presence of its typical IR bands: ν (C=C), i.e., 1600 and 1570 cm^{-1} (8a and 8b stretching mode), 1490 and 1450 cm^{-1} (19a and 19b stretching mode); δ (CH_3), i.e., 1370 cm^{-1}; δ (C–OH), i.e., 1206 cm^{-1}; ν (C–O), i.e., 1150–1075 cm^{-1}.

To study the interaction between the alcohol alone and the sites exposed at the catalyst surface, FT-IR analyses of 1-phenylethanol adsorbed on AuTiDeg and of the liquid film were carried out. The results (see Fig. S5, section a in Supplementary Material) highlight that the alcohol interacts, via H-bonding, only with the OH groups, exposed at the titania surface.

The effect of oxygen on pre-adsorbed alcohol is already evident at room temperature (Fig. 2, dotted and fine lines a and b). In fact, the oxidation reaction of the alcohol to ketone is confirmed by the presence of the band at 1670 cm^{-1}, related to the C=O stretching and another at 1281 cm^{-1} which is typical of C–C phenyl–carbonyl stretching. Interestingly, the C=O stretching band is split into two components that are well noticeable in the spectrum of alcohol/toluene–O_2 interaction (fine line b).

In this case, the comparison of FT-IR spectra of the acetophenone liquid film and of the acetophenone adsorbed on Au/TiO_2 (Fig. S4, section b) indicated that the ketone molecule is adsorbed onto the support surface, giving rise to a complex band in the carbonyl stretching region, while no interaction between the ketone and gold sites is evident as confirmed by the spectra of acetophenone adsorbed on P25 (see Fig. S6 in Supplementary Material).

The spectra collected at r.t., after heating at 80 °C in the presence of alcohol–O_2 and at 110 °C in alcohol/toluene–O_2 mixtures (Fig. 2, dashed lines, a and b, respectively), show an increase of the band intensity related to acetophenone and a simultaneous decrease of the band intensity related to 1-phenylethanol, e.g., δ (C–OH), and ν (C–O), at 1206 cm^{-1} and 1150–1075 cm^{-1}, respectively. These further confirm the reactivity of the catalyst toward alcohol oxidation.

Starting from these results, with the aim to investigate the nature of the active sites and the role played by the oxygen, FT-IR investigations have been performed on Au/TiO_2 submitted both to an oxidizing (in O_2 at 400 °C) and to a reducing (in H_2 at 200 °C) treatment. These thermal treatments produce Au sites with different oxidation states

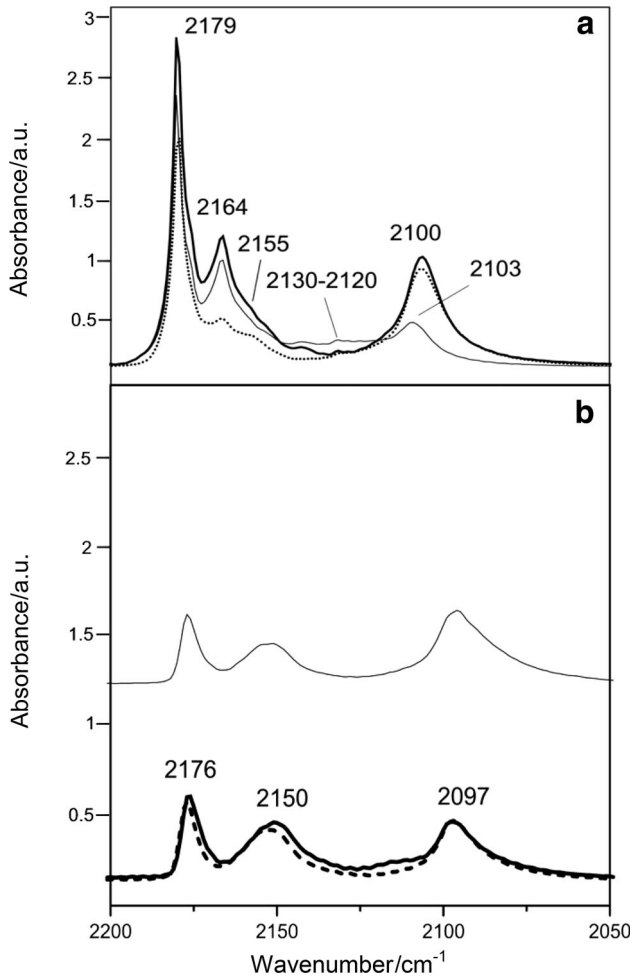

Fig. 1 **a** FT-IR spectra of CO adsorbed at −153 °C on AuTiRed (*solid line*), $AuTiO_x$ (*fine line*), and AuTiDeg (*dotted line*). **b** FT-IR spectra of CO adsorbed at −153 °C, after 1-phenylethanol-O_2 interaction on AuTiRed (*bold line*) and $AuTiO_x$ (*dashed line*). *Fine line* spectrum of CO adsorbed on AuTiRed after the interaction between alcohol and pre-adsorbed oxygen

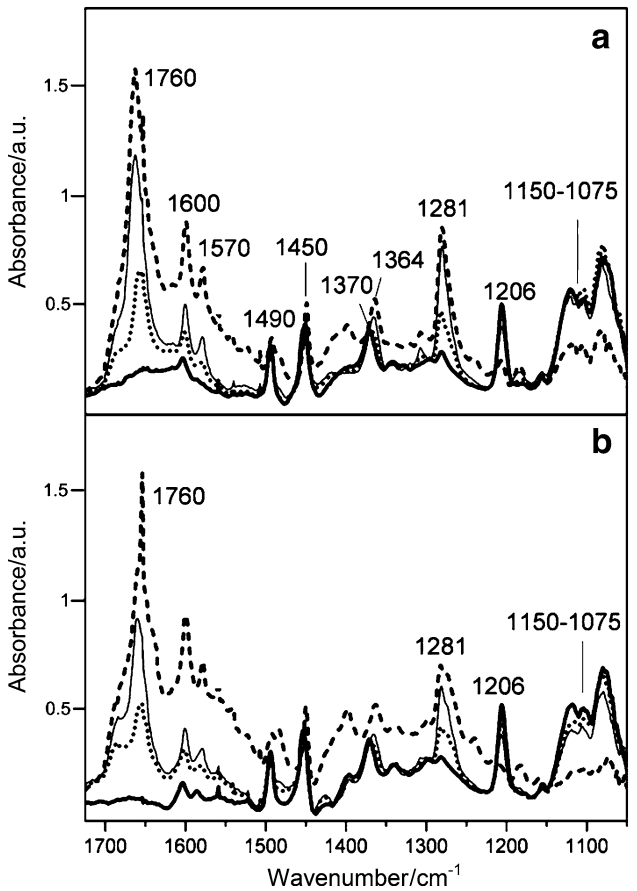

Fig. 2 FT-IR spectra of 1-phenylethanol–O_2 interaction (**a**) and of 1-phenylethanol/toluene–O_2 interaction (**b**) on AuTiDeg surface. *Solid lines* adsorbed alcohol or alcohol/toluene. *Dotted lines* after O_2 inlet. *Fine line* after 30 min of O_2 interaction. *Dashed lines* mixture heated at 80 °C (**a**) and at 110 °C (**b**)

(Fig. 1a). We, therefore, wish to stress that, despite the catalyst is not activated in this way before the catalytic test, this FT-IR study allows us to explore the active sites behavior when Au^0 or $Au^{\delta+}$ sites are exposed on the catalyst surface.

The FT-IR experiments were undertaken at r.t. with a vapor pressure of 0.5 mbar of 1-phenylethanol. In Fig. 3a, the spectra collected after 10 min of interaction between the alcohol and the differently treated catalyst are reported.

As reported above, the adsorption of 1-phenylethanol onto the catalyst surface is confirmed by the presence of typical IR bands, i.e., ν (C=C) (1495 and 1450 cm^{-1}), δ (CH_3) (1370 cm^{-1}), δ (C–OH) (1205 cm^{-1}) and ν (C–O) (1120–1075 cm^{-1}), ν (CH_2) and ν (CH_3; 3100–2860 cm^{-1}). Interestingly, a very large absorption centered at 3300 cm^{-1} and a band at 1630 cm^{-1} are present in both samples. This is congruent to the formation of water, which remains adsorbed on the catalyst surface. In addition, a new peak, typical of OH bridged groups, appeared at 3696 cm^{-1}. Water formation in the oxidation reaction of cyclohexanol and 2-cyclohexen-1-ol on Au(111) was confirmed by Friend et al. [31], due to the extraction of the two H atoms of the alcohol by Au–O species.

If we consider that Au nanoparticles are supported on TiO_2 and that the water formation also occurs on the reduced catalyst without the presence of O_2, it should be clear that the support has a direct role, as reported by Gonzalez-Yanez et al. [32] in their study of the surface reactions of ethanol on an Au/TiO_2 catalyst.

However, to have experimental data on the mechanism of water formation on the surface of the catalyst used in this study, the same IR experiment was undertaken on the bare P25 support reduced in H_2 at 200 °C, and on reduced and deuterated P25 (see Fig. S7 in Supplementary

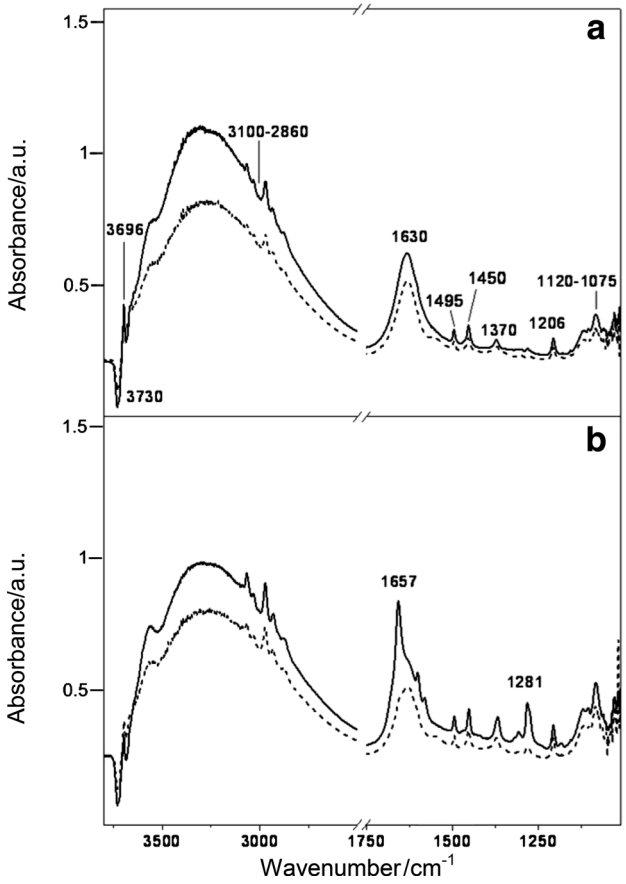

Fig. 3 FT-IR spectra of 1-phenylethanol adsorption on AuTiRed (*solid line*) and $AuTiO_x$ (*dashed line*). **a** After the interaction with 0.5 mbar 1-phenylethanol. **b** After 30 mbar O_2 on adsorbed 1-phenylethanol

Material). Interestingly, the frequency of the adsorbed H_2O bands and of bridged OH groups on Au/TiO_2 is shifted 10 cm^{-1} to higher frequency as compared to those observed on bare P25. This may be an indication of adsorbed sites with different chemical surroundings (support sites in close contact with Au nanoparticles, for example).

Moreover, considering that this reactivity is totally absent on AuTiDeg (Fig. 2a, b, solid lines), and that linear OH groups are involved in H-bond with residual water on this sample (Fig. S1, section a), it is possible to conclude that water formation is due to the reaction of alcohol with these linear hydroxyls.

Actually, the mechanism of gold-catalyzed alcohol oxidation is not completely clear. Friend and co-workers have reported the importance of the Au–O species, [27, 31] also in other reaction types [33]. On the other hand, Corma et al. [17] have proposed Au–H intermediate formation as the key step in aerobic alcohol oxidation, limiting the role of oxygen to the regeneration of the catalysts. This is also asserted by Conte et al. [34] via the combined use of EPR spectroscopy and spin trapping techniques. In addition, the authors pointed out that alcohol oxidation proceeds via a radical mechanism.

The absence of a band related to C=O stretching in the spectra reported in Fig. 3a, clearly shows that the interaction of 1-phenylethanol, at r.t., with the oxidized or reduced catalyst does not produce any oxidation product, in our experimental conditions.

Most probably, in our conditions, the oxidation reaction does not follow the Au–H intermediate formation pathway. Indeed oxygen is needed for alcohol oxidation, as demonstrated when we performed the catalytic test under nitrogen flow (Table 1; entry 6). Therefore, the effect of oxygen on pre-adsorbed 1-phenylethanol was investigated at r.t., and the results are shown in Fig. 3b.

The first effect is the intensification of the bands related to 1-phenylethanol across the whole range. This manifestation can be attributed to the increase of the pressure inside the IR cell, due to the inlet of O_2 on pre-adsorbed alcohol. The alcohol oxidation reaction on the catalyst surface is confirmed by the presence of the band at 1657 cm^{-1}, related to C=O stretching and another at 1281 cm^{-1}, typical of phenyl–carbonyl C–C stretching, in the AuTiRed spectrum (solid line).

Acetophenone formation is the important proof that oxygen is needed for the alcohol oxidation in our case, because Au–O species are the active sites promoting the C–H bond scission, in accordance with the reaction mechanism proposed by Friend and co-workers. Considering both this latter statement and the results of the FTIR experiment with CO at low temperature on $AuTiO_x$ (Fig. 1a, fine line) that revealed the presence of Au-O species located at metal-support interface, we would expect the ketone formation on this sample, even before the O_2 inlet. Surprisingly, however, acetophenone formation is inhibited on the oxidized catalyst.

Green and co-workers [35] have recently reported that the oxidation reactions are catalyzed by the dissociation of O_2 on borderline sites on Au/TiO_2 catalyst (Au–O–Ti) which involve both Au and Ti^{4+} centers, located at the interface between the Au nanoparticles and the TiO_2 support. The same authors [36] have also highlighted, in the case of CO oxidation, a significant reaction inhibition when the Au/TiO_2 catalyst is pre-oxidized. In this case, both their theoretical DFT calculations and experimental results revealed that chemisorbed oxygen atoms induce a positive charge in the adjacent Au atoms, doubling the activation energy for CO oxidation at the borderline sites.

Hong and Rahman [37] have recently reported the high activity of interfacial sites of the Au_{13}/TiO_2 (110) model system in methanol decomposition. Their theoretical studies have highlighted that this high activity is closely related to the important charge-transfer-induced Coulomb

interaction between the gold and the support in the Au–O–Ti dual perimeter sites. Therefore, the formation of a strong O–Au bond between gold and methoxy occurs in such sites, leading to a weakening of the molecular C–O bond and to a repulsive interaction between the partially positive gold and the carbon atom bound to the oxygen. These effects contribute to enhance the reactivity of methoxy via the extraction of H atom, toward CH_2O formation.

With our experimental results and these literature information in mind, we can assert that these sites, located at the interface between the Au nanoparticles and the TiO_2 support, play a crucial role in acetophenone formation. In particular, the lack of oxidation product on the $AuTiO_x$ sample, both in the presence and in the absence of oxygen, can be explained by the existence of an Au-O bond on borderline sites (Fig. 1a, fine line) that makes them not available for the activation of the 1-phenylethoxy species. Therefore, the oxidation reaction is inhibited on the pre-oxidized samples.

To further sustain this statement, the oxidation reaction was repeated on AuTiRed, and the effect of 1-phenylethanol at r.t. on pre-adsorbed O_2 was studied. As previously reported in the literature [38], the effect of oxygen is to re-oxidize a reduced Au/TiO_2 catalyst, even at low temperature. In our case, the spectrum collected after the inlet of alcohol on pre-adsorbed oxygen (see Fig. S8 in Supplementary Material) is quite similar to what was observed on $AuTiO_x$ (Fig. 3b, dashed line), thus confirming the negative effect of oxygen chemisorbed on Au atoms before alcohol adsorption.

At this point, it is important to stress that, if the oxidation of 1-phenylethanol was carried out in conditions close to those used for FTIR experiments (i.e., in oxygen flow in absence of the base), the alcohol was not completely oxidized (see Table 1; entry 9) even when bubble a continuous oxygen flow through the reaction. Therefore, the addition of a strong base (NaOH) was necessary to obtain the complete oxidation of 1-phenylethanol to acetophenone (Table 1; entry 10).

In the light of this, we can assert that: (1) since acetophenone forms at the beginning of the oxidation reaction, the sites needed for alcohol activation are available on catalyst surface; (2) since the complete oxidation of 1-phenylethanol does not occur, many of these sites are depleted in some way. In fact, only adding NaOH the oxidation reaction ends.

We can tentatively explain this as follows: since the OH groups, present on titania, are depleted after the H alcohol group extraction (thus producing water in the first step), O–H bond scission can be promoted by further interaction between the base and the hydroxyl groups.

The stability and, if carried out, the recycling of catalysts are two of the main topics in the field of heterogeneous catalysis. We demonstrated (see Tables A and B in Supplementary Material) that Au/TiO_2 can be reused up to the sixth consecutive run without any loss in its catalytic effectiveness. However, a study of the surface site situation after a catalytic reaction can be useful to make considerations about the deactivation process and, as a consequence, to set up a cleaning procedure to recycle the catalysts.

With this in mind, FT-IR experiments of CO adsorbed at low temperature after the 1-phenylethanol–O_2 interaction were undertaken as a first step, both on AuTiRed and on $AuTiO_x$ that had been simply outgassed for 30 min at r.t. It is important to stress that outgassing at r.t. is not sufficient to completely eliminate both ketone and alcohol, because of their strong interaction with support surface sites.

In Fig. 1b, the FT-IR spectra of AuTiRed (bold line) and of $AuTiO_x$ (dashed line) are reported. Moreover, the spectrum of adsorbed CO on AuTiRed (fine line) after the interaction between the alcohol and the pre-adsorbed oxygen is also shown for comparison.

Firstly, the most interesting feature here is that all the spectra are quite similar, showing the same surface site distribution after the reaction, despite having different reactivity. Moreover, this also occurs when the order of reactants is reversed, as shown by the spectrum of CO adsorbed on AuTiRed after the interaction between alcohol and pre-adsorbed oxygen (fine line).

In addition, a comparison with the spectra of adsorbed CO, collected before the 1-phenylethanol-O_2 interaction on AuTiRed (Fig. 1a, solid line) and on $AuTiO_x$ (Fig. 1a, fine line) shows that:

1. a decrease in the intensity of the band related to CO–Au sites interaction occurs in the AuTiRed spectrum (Fig. 1b, bold line). As we have FTIR evidence that both ketone and alcohol are not adsorbed onto Au sites, we can tentatively explain this feature with the presence of residual acetophenone and 1-phenylethanol adsorbed onto the support surface near the Au sites, which makes the diffusion of CO molecules towards the gold sites difficult.
2. the band due to oxidized gold sites, i.e., in the 2130–2120 cm^{-1} range, disappears in the $AuTiO_x$ spectrum (Fig. 1b, fine line), indicating that there is no more oxygen bounded on the Au borderline sites, even if FT-IR measurements did not show reactivity on this sample.

A further validation of this latter point can be found in FTIR spectra of the alcohol oxidation being carried out again on the "used" $AuTiO_x$ (see Fig. S9 in Supplementary Material). The presence of a band at 1658 cm^{-1}, due to ketone C=O stretching after the adsorption of 1-phenylethanol can be considered evidence of the simultaneous

presence of "free" Au at the Au–TiO_2 interface, where the activation of the alcohol occurs, and residual active oxygen adsorbed on Au sites, located on non-borderline positions. Moreover, the effect of a new O_2 inlet on the pre-adsorbed alcohol is to further improve the oxidation reaction, as shown by the intensity increase in the C=O stretching band. Therefore, the question is: how has the oxygen been removed from the Au borderline sites?

Coming back to our $AuTiO_x$ experimental results, it is worth noting that FT-IR experiment of adsorbed 1-phenylethanol (Fig. 3a, dashed line) has shown water production, adsorbed onto support sites in close contact with Au nanoparticles. The interaction between co-adsorbed H_2O and oxygen has been highlighted by theoretical studies [39, 40], which have revealed the formation of co-adsorbed complexes which are strongly bound to gold clusters. In addition, other works have reported an increase in oxygen mobility on reducible supports in the presence of surface water [41, 42]. The promotion effect of water on the catalytic activity of Au/TiO_2 has also been demonstrated by Yang et al. [19] in the selective oxidation of benzyl alcohol to benzaldehyde and by Aghaei and Berger [43] in the selective oxidation of aqueous ethanol solution. These results clearly demonstrate the strong interaction between water and oxygen adsorbed onto the catalyst surface. Considering our experimental data, along with the relevant literature information, we tentatively explain the disappearance of the oxygen bound onto Au borderline sites as a result of an interaction with adsorbed H_2O that probably promotes oxygen spill-over on the support surface.

In the light of these, we can assert that, under our experimental conditions, alcohol group H extraction is carried out by OH groups and O_2-basic sites present on titania and the product water was adsorbed onto the support surface. The formed alkoxy species is then activated on Au sites (Au–O–Ti), located at the interface of the Au nanoparticles and the TiO_2, and C–H bond scission is promoted by the active oxygen species (Au–O), generated by O_2 dissociation on Au nanoparticles. Scheme 1 shows a withdrawing of the reaction steps.

Oxidation reaction of benzylic (1e-1i) and primary alcohols (1j-1k)

Benzylic and primary alcohols were also reacted to further expand the scope of our work. The oxidation of benzyl alcohol (**1e**) was initially carried out in the same conditions used for the oxidation of 1-phenylethanol (**1a**). As already observed for **1a**, oxidation did not take place without a base (Table 3; entry 1) and NaOH was, therefore, added to the reaction mixture.

Unfortunately, we only observed the total decomposition of **1a** (Table 3, entry 2), probably due to the interaction of the strong base with relatively acidic methylenic protons. K_2CO_3 was, therefore, used (Table 3, entry 3) and, interestingly, benzaldehyde (**3a**) was obtained in good yields as well as by-product benzyl benzoate (**4a**).

Surprisingly, K_2CO_3 is able to deprotonate the very weak acid **1e** despite it being a much weaker base than NaOH. Since we also observed that the activation of the

Scheme 1

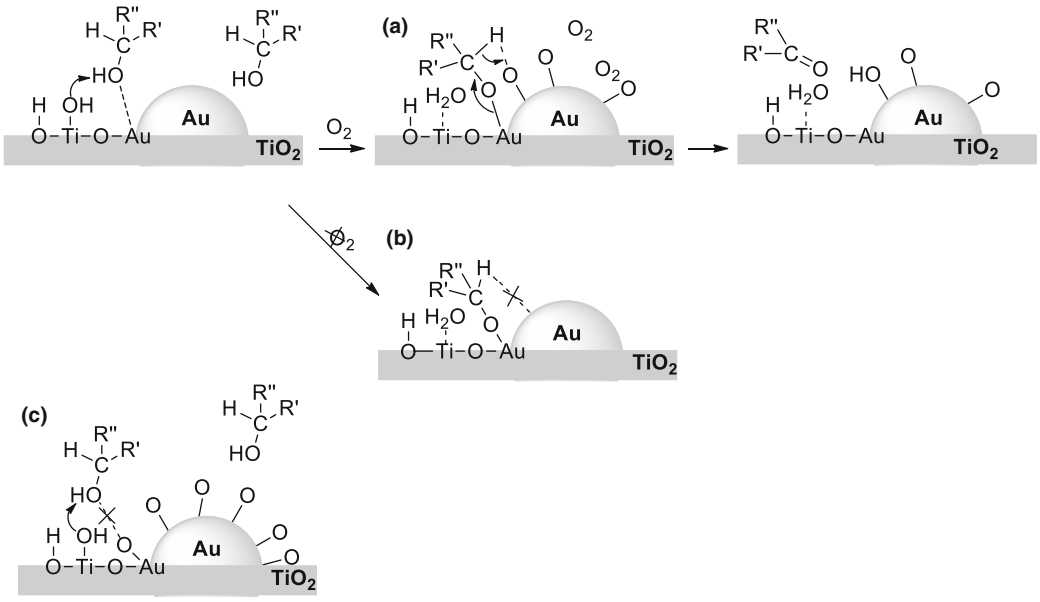

Table 3 Oxidation of benzylic alcohol **1e**

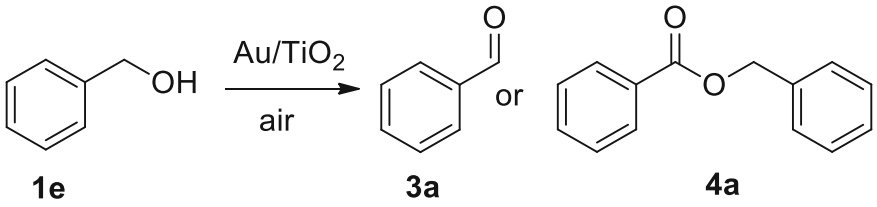

Entry	Solvent	Base	*T*/°C	Time/h	Yield/% of **3a**	Yield/% of **4a**[a, b]
1	Toluene	–	110	24	–[c]	–
2	Toluene	NaOH (3 eq.)	110	24	–[d]	–
3	Toluene	K_2CO_3 (6 eq.)[e]	110	15	83[f]	17
4	–	K_2CO_3 (6 eq.)[g]	80	20	–	97[f, h]

[a] All the reactions were carried out with 1 mmol of **1e**, 3 or 6 mmol of base, and 50 mg of Au/TiO_2 (equal to 15 mol % of Au)

[b] Yields refer to the pure and isolated **3a** or **4a**

[c] Unreacted **1e** was only recovered

[d] Total decomposition of **1e** was observed

[e] Using Na_2CO_3, the yield of **3a** was lower (60 %). Also using 3 mmol of K_2CO_3, the yield was considerably lower (18 %); [f] the conversion was total

[g] With lesser amounts of base, the reaction was not complete

[h] The reaction carried out at 110 °C gave lower yield of **4a** (52 %)

alcohol on Au sites (Au–O–Ti) located at the Au–TiO_2 interface is essential, we can assume that this interaction facilitates proton extraction by K_2CO_3 by weakening the OH bond of the alcohol group. Moreover, proton extraction from alcohol groups was also performed by OH groups and O_2-basic sites present on titania, producing water adsorbed on the support surface, as we have demonstrated. According to these observations, we can consider that the combined action of TiO_2 and K_2CO_3 was essential to initializing the oxidation reaction of **1e**.

Taking into account these observations, we propose the benzaldehyde formation reaction pathway as shown in Scheme 2 (most probably the steps showed in the scheme are simultaneous). Interestingly, only **4a** was obtained in excellent yield (98 %) when the reaction was performed without toluene (Table 3, entry 4). It is reasonable to assume the formation of **4a** due to the alcoholate's nucleophilic attack on the aldehyde. This reaction may be promoted by the activation of the benzaldehyde carbonyl group on the catalyst surface.

To validate this hypothesis, we have studied the nature of the interaction between the benzaldehyde and the catalyst by FTIR spectroscopy. The FTIR spectra of the aldehyde adsorbed on AuTiDeg and on P25 (see Fig S10 in Supplementary Material) indicate that the molecule is adsorbed onto the support sites, without any evidence of an interaction between the benzaldehyde and gold sites.

These results suggest that benzyl benzoate formation follows the pathway reported in the Scheme 3; the alcoholate is adsorbed onto Au borderline sites, while the benzaldehyde interacts through the carbonyl group with the Ti^{4+} sites neighboring the gold nanoparticles. This interaction makes the carbonyl group more available to the nucleophilic attack of the alcoholate.

After optimizing the reaction conditions, other benzylic alcohols and primary alcohols were reacted. The results are shown in Table 4. First of all, aldehydes **3b–3f** (Table 4; entries 1, 3, 5, 7) or esters **4b–4d**, **4f** (Table 4; entries 2, 4, 6) were selectively obtained from benzylic alcohols **1f–1k**, depended on the presence or the absence of the solvent, respectively. Moreover, it is interesting to note that the different electronic effects of the substituent bound to the aromatic ring did not influence the progress of the reaction. Corma et al. [17] have proposed a reaction mechanism in which the breaking of benzylic CH bond was faster than the formation of the CO π bond, so that a partial positive transition state was assumed.

Their hypothesis was confirmed by the fact that benzylic alcohols bearing electron donating groups were oxidized faster than those bearing electron-withdrawing groups. However, the results reported in Table 4 certainly confirm that no cationic or partially cationic intermediate is feasible in our case, since the formation of the CO group π bond and the breakage of CH bond are almost simultaneous (Scheme 1b).

Table 4 Oxidation of benzyl **1f–1i** and primary alcohols **1j**, **1k**

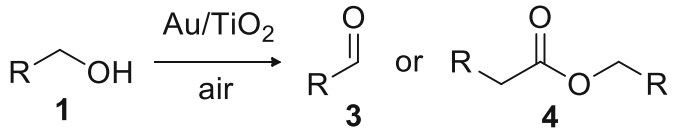

Entry	R	Solvent	*T*/°C	Time/h	Yield/% of **3**	Yield/% of **4**[a, b]
1	4-MeC_6H_4 (**1f**)	Toluene	110	48	92[c] (**3b**)	Traces (**4b**)
2	4-MeC_6H_4 (**1f**)	–	80	24	–	87[c, d] (**4b**)
3	4-$MeOC_6H_4$ (**1g**)	Toluene	110	24	95[c] (**3c**)	Traces (**4c**)
4	4-$MeOC_6H_4$ (**1g**)	–	80	24	–	89[c, d] (**4b**)
5	4-ClC_6H_4 (**1h**)	Toluene	110	24	89[c] (**3d**)	Traces (**4d**)
6	4-ClC_6H_4 (**1h**)	–	80	24	–	88[c, d] (**4b**)
7	4-$NO_2C_6H_4$ (**1i**)	Toluene	110	24	60[c] (**3e**)	–
8	4-$NO_2C_6H_4$ (**1i**)	–	80	24	–	–[c, e] (**4e**)
9	C_6H_5CH=CH (**1j**)	Toluene	110	24	93[c] (**3e**)	–
10	nC_5H_{11} (**1k**)	Toluene	110	72	–	–
11	nC_5H_{11} (**1k**)	–	80	48	–	90[c, d] (**4f**)

[a] All the reactions were carried out with 1 mmol of **1**, 6 mmol of K_2CO_3, and 50 mg of Au/TiO_2 (equal to 15 mol % of Au)

[b] Yields refer to the pure and isolated **3** or **4**

[c] The conversion was total

[d] The reactions carried out at 110 °C gave lower yield of **4**

[e] GC and GC–MS analyses of the crude residue showed the presence of **4e** (m/z = 302, M^+). However, it was not possible to isolate it with adequate purity

Scheme 2

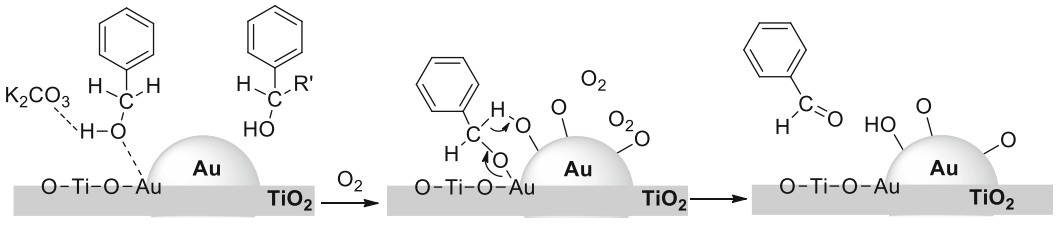

Moreover, the alcohol oxidation reaction was chemoselective, and the cinnamyl alcohol (**1j**) double bond remained unchanged at the end of the reaction (Table 4; entry 9). In addition, the oxidation of hexan-1-ol (**1k**) allowed us to obtain **4f** only (Table 4; entry 11). In fact, the reaction that was carried out in toluene failed (Table 4; entry 10). It is likely that hexanal (**3g**) spontaneously decomposed in these conditions. We excluded its further oxidation because we did not recover the corresponding carboxylic acid; its thermal decomposition seemed more probable [44].

FT-IR characterization

To understand why the presence/absence of the solvent influences the selectivity of the oxidation reaction, FT-IR experiments of toluene adsorbed were undertaken at r.t. on AuTiDeg. The C–H stretching mode region of the spectra is shown in Fig. 4a.

The spectrum of toluene adsorbed onto the catalyst at r.t. (bold curve) shows multiple bands in the 3100–3000 cm^{-1} region attributable to aromatic C–H stretching vibrations, while the methyl group has typical bands near 2925 and

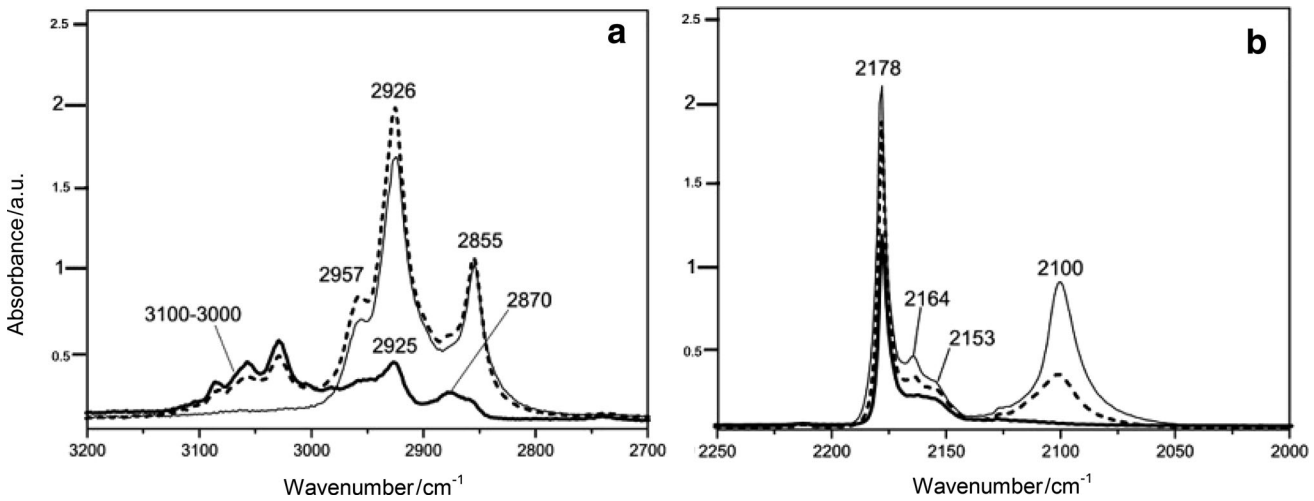

Fig. 4 **a** FT-IR spectra of toluene adsorbed on AuTiDeg at r.t. (*bold curve*), heated at 110 °C (*dotted curve*) and outgassed 30 min at r.t. (*fine curve*). **b** FT-IR spectra of CO adsorbed at −153 °C on AuTiDeg before the interaction with toluene (*fine curve*), after the interaction with the solvent at r.t. (*dotted curve*) and after heating in toluene at 110 °C (*bold curve*)

2870 cm^{-1} both attributable to the symmetric CH_3 stretching mode.

After heating in toluene at 110 °C (dotted curve), no difference was observed in the aromatic stretching region while the bands in the aliphatic stretching one show an intensity increase and, more interestingly, they are irreversible to outgassing (fine curve).

Since the same experiment carried out on P25 did not reveal any change in the spectrum (data not shown for the sake of brevity), these features provide evidence of gold nanoparticles having an effect on toluene molecules. In particular, the peak at 2855 cm^{-1} can be attributed to the symmetric stretching vibration of CH_2 groups. Even if it is not easy to associate these multiple bands to a specific compound, their relative intensity is comparable to that observed in the spectrum of methylcyclohexane [45]. The effect of the interaction between toluene and the surface sites was investigated using CO as a probe molecule, adsorbed at low temperature. A comparison of the spectra collected before and after the interaction with the solvent (Fig. 4b) has revealed a decrease in intensity of the band related to the CO–Au (2100 cm^{-1}) and CO–Ti^{4+} interaction (2180–2150 cm^{-1}).

In the light of this, we assume that toluene and aliphatic compounds (derived from it) are adsorbed onto the support surface near the Au sites which makes the diffusion of the CO molecules towards the gold sites difficult.

These findings can explain the different selectivity that occurs in the presence or absence of toluene. Indeed, the presence of compounds adsorbed on Ti^{4+} sites neighboring to the gold nanoparticles makes these sites not available for the activation of the carbonyl group of the aldehyde (as shown in the Scheme 3). This means why benzaldehyde is the main product of the benzyl alcohol oxidation in the presence of the solvent.

Conclusions

From the synthetic point of view, we proposed here an efficient and easy method to oxidize primary, benzylic, or secondary alcohols on a commercial Au/TiO_2 catalyst in the presence of atmospheric oxygen under relatively mild and neat conditions.

FT-IR investigations highlighted both the role of borderline sites (Au–O–Ti), located at the Au nanoparticles-TiO_2 support interface, in the activation of the alcohoxy species, and the role of the active oxygen species (Au–O) which is generated by O_2 dissociation on Au nanoparticles, in C–H bond scission and demonstrated that, in our experimental conditions, "free" Au sites, located at Au–TiO_2 interface, and Au–O species are necessary to perform the selective oxidation of the alcohols on commercial Au/TiO_2.

Experimental section

The catalyst used in this study was a commercial AUROlite™ sample (Au/TiO_2) purchased from STREM Chemicals (please see: http://www.strem.com/catalog/v/79-0165/25/gold_7440-57-5). The sample was prepared to support gold nanoparticles, on TiO_2 (P25 Degussa) extrudates, with a specific surface area (SSA) of 40–50 m^2/g. The gold loading is 1 % wt and the catalyst was pretreated by the manufacturer to ensure that Au particle average size was 2–3 nm. Furthermore, this catalyst was characterized and tested in other catalytic reactions, such as CO oxidation [46].

The catalyst was used "as received", without any pretreatment. Analytical grade reagents and solvents were used and reactions were monitored by GC and GC–MS. Petroleum ether refers to the fraction boiling in the range

Scheme 3

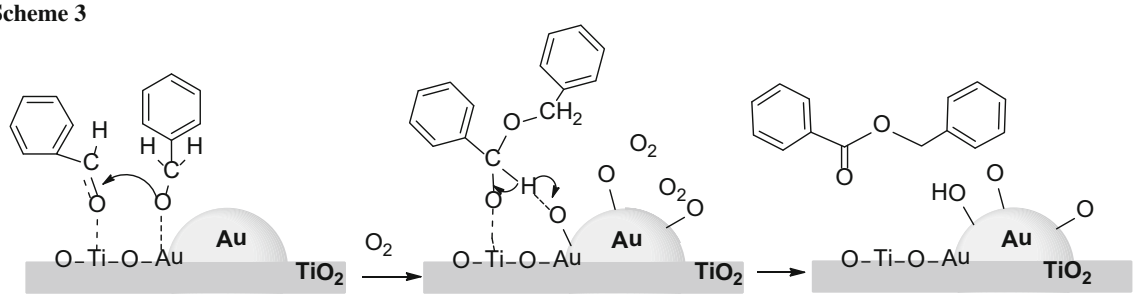

40–70 °C. All reagents were purchased from Sigma-Aldrich. Unless otherwise stated, all the reactions were performed in opened air flasks.

The structures and purity of the products of the oxidation of secondary alcohols, namely acetophenone (**2a**), benzophenone (**2b**), and cyclohexanone (**2c**), were confirmed by comparison of their physical and spectral data with those of a commercial sample (Sigma-Aldrich). Also the structures and purity of the products of the oxidation of benzylic and primary alcohols, namely benzaldehyde (**3a**), 4-methylbenzaldehyde (**3b**), 4-methoxybenzaldehyde (**3c**), 4-chlorobenzaldehyde (**3d**), 4-nitrobenzaldehyde (**3e**), *trans*-cinnamaldehyde (**3f**), benzyl benzoate (**4a**), and hexyl hexanoate (**4f**), were confirmed by comparison of their physical and spectral data with those of a commercial sample (Sigma-Aldrich); 4-methylbenzyl 4′-methylbenzoate (**4b**) [47], 4-methoxybenzyl 4′-methoxybenzoate (**4c**) [47], 4-chlorobenzyl 4′-chlorobenzoate (**4d**) [48] with those reported in the literature.

^{1}H NMR spectra were recorded on a Bruker Avance 200 spectrometer at 200 MHz. Mass spectra were recorded on an HP 5989B mass selective detector connected to an HP 5890 GC with cross-linked methyl silicone capillary column. High purity grade gases (H_2, CO, O_2) were used for sample pretreatments and FTIR experiments. Sample characterization, FTIR experiments details and synthetic procedures of the catalytic tests are reported in Supplementary Material.

Acknowledgments This work was supported by the University of Torino and by Ministero dell'Università e della Ricerca.

References

1. Haruta M (2005) Nature 437:1098
2. Hayashi T, Tanaka K, Haruta M (1998) J Catal 78:566
3. Haruta M, Date M (2001) Appl Catal A-Gen 222:427
4. Prati L, Rossi M (1998) J Catal 176:552
5. Okumura M, Akita T, Haruta M (2002) Catal Today 74:265
6. Piccolo L, Piednoir A, Bertolini JC (2005) Surf Sci 592:169
7. Bailie JE, Hutchings GJ (1999) Chem Comm 2151
8. Claus P, Bruckner A, Mohr C, Hofmeister H (2000) J Am Chem Soc 122:11430
9. Gonzalez-Arellano C, Corma A, Iglesias M, Sanchez F (2006) J Catal 238:497
10. Gonzalez-Arellano C, Abad A, Corma A, Garcia H, Iglesias M, Sanchez F (2007) Angew Chem Int Ed 46:1536
11. Carrettin S, Concepcion P, Corma A, Nieto JML, Puntes VF (2004) Angew Chem Int Ed 43:2538
12. Han J, Liu Y, Guo R (2009) J Am Chem Soc 131:2060
13. Hashmi ASK, Hutchings GJ (2006) Angew Chem Int Ed 45:7896
14. Corma A, Garcia H (2008) Chem Soc Rev 37:2096
15. Zhang Y, Cui X, Shi F, Deng Y (2012) Chem Rev 112:2467
16. Dimitratos N, Lopez-Sanchez JA, Hutchings GJ (2012) Chem Sci 3:20
17. Abad A, Corma A, Garcia H (2008) Chem Eur J 14:212
18. Bianchi C, Porta F, Prati L, Rossi M (2000) Top Catal 13:231
19. Yang X, Wang X, Liang C, Su W, Wang C, Feng Z, Li C, Qiu J (2008) Catal Comm 9:2278
20. Martinez-Gonzalez S, Gomez-Aviles A, Martynyuk O, Pestryakov A, Bogdanchikova N, Cortes Corberan V (2014) Catal Today 227:65
21. Zhao J, Liu H, Ye S, Cui Y, Xue N, Peng L, Guo X, Ding V (2013) Nanoscale 5:9546
22. Villa A, Chan-Thaw CE, Veith GM, More KL, Ferri D, Prati L (2011) ChemCatChem 3:1612
23. Villa A, Wang D, Veith GM, Vindigni F, Prati L (2013) Catal Sci Tech 3:3036
24. Costa VV, Estrada M, Demidova Y, Prosvirin I, Kriventsov V, Cotta RF, Fuentes S, Simakov A, Gusevskaya EV (2012) J Catal 292:148
25. Estrada M, Costa VV, Beloshapkin S, Fuentes S, Stoyanov E, Gusevskaya EV, Simakov A (2014) Appl Catal A-Gen 473:96
26. Simakova OA, Smolentseva E, Estrada M, Murzina EV, Beloshapkin S, Willför SM, Simakov AV, Murzin DY (2012) J Catal 291:95
27. Baker TA, Liu X, Friend CM (2011) Phys Chem Chem Phys 13:34
28. Panayotov DA, Burrows SP, Yates JT Jr, Morris JR (2011) J Phys Chem C 115:22400
29. Hadjiivanov K, Lamotte J, Lavalley JC (1997) Langmuir 13:3374
30. Boccuzzi F, Chiorino A, Tsubota S, Haruta M (1996) J Phys Chem 100:3625
31. Liu X, Friend CM (2010) Langmuir 26:16552
32. Gonzalez-Yanez EO, Fuentes GA, Hernandez-Teran ME, Fierro-Gonzalez JC (2013) Appl Catal A-Gen 464:374
33. Xu B, Haubrich J, Freyschlag CG, Madix RJ, Friend CM (2010) Chem Sci 1:310
34. Conte M, Miyamura H, Kobayashi S, Chechik V (2009) J Am Chem Soc 131:7189

35. Green IX, Tang WJ, Neurock M, Yates JT Jr (2011) Science 333:736
36. Green IX, Tang WJ, McEntee M, Neurock M, Yates JT Jr (2012) J Am Chem Soc 134:12717
37. Hong S, Rahman TS (2013) J Am Chem Soc 135:7629
38. Boccuzzi F, Chiorino A, Manzoli M, Lu P, Akita T, Ichikawa S, Haruta M (2001) J Catal 202:256
39. Bongiorno A, Landman U (2005) Phys Rev Lett 95:106102
40. Liu LM, McAllister B, Ye HQ, Hu P (2006) J Am Chem Soc 128:4017
41. Pozdnyakova-Tellinger O, Teschner D, Kroehnert J, Jentoft FC, Knop-Gericke A, Schlogl R, Wootsch A (2007) J Phys Chem C 111:5426
42. Teschner D, Wootsch A, Pozdnyakova-Tellinger O, Krohnert J, Vass EM, Havecker M, Zafeiratos S, Schnorch P, Jentoft PC, Knop-Gericke A, Schlogl R (2007) J Catal 249:318
43. Aghaei P, Berger RJ (2013) Appl Catal B-Env 132:195
44. Ho SK (1963) Proc R Soc London Ser A 276:278
45. Colthup NB, Daly LH, Wiberly SE (1975) Introduction to infrared and Raman spectroscopy, 2nd edn. Academic Press, New York, p 220
46. Walther G, Mowbray DJ, Jiang T, Jones G, Jensen S, Quaade UJ, Horch S (2008) J Catal 260:86
47. Simon M-O, Darses S (2010) Adv Synth Catal 352:305
48. Cronin L, Manoni F, O'Connor CJ, Connon SJ (2010) Angew Chem Int Ed 49:3045
49. Saavedra J, Powell C, Panthi B, Pursell CJ, Chandler BD (2013) J Catal 307:37